Journal of Scientific Computing, Vol. 5, No. 4, 1990

An Operator-Integration-Factor Splitting Method for Time-Dependent Problems: Application to Incompressible Fluid Flow

Y. Maday,[1] Anthony T. Patera,[2] and Einar M. Rønquist[3]

Received November 9, 1990

In this paper we present a simple, general methodology for the generation of high-order operator decomposition ("splitting") techniques for the solution of time-dependent problems arising in ordinary and partial differential equations. The new approach exploits operator integration factors to reduce multiple-operator equations to an associated series of single-operator initial-value subproblems. Two illustrations of the procedure are presented: the first, a second-order method in time applied to velocity–pressure decoupling in the incompressible Stokes problem; the second, a third-order method in time applied to convection-Stokes decoupling in the incompressible Navier–Stokes equations. Critical open questions are briefly described.

KEY WORDS: Splitting methods; operator decomposition; Navier–Stokes equations; pressure.

1. INTRODUCTION

In this article we introduce a new methodology for the development of simple, high-order operator-decomposition (or "splitting") techniques (Strang, 1968; Marchuk, 1971; Yanenko, 1971) for the solution of time-dependent differential equations. We consider the general initial-value problem,

$$\frac{d\underline{u}}{dt} = \underline{A}(t)\,\underline{u} + \underline{B}(t)\,\underline{u} + \underline{f}(t), \qquad 0 < t < T \tag{1.1}$$

with initial conditions $\underline{u}(t=0) = \underline{u}_0$. Here $\underline{u} \in \mathcal{R}^{\mathcal{N}}$ is the solution vector, t

[1] Analyse Numérique, Université Pierre et Marie Curie, Paris, France.
[2] Department of Mechanical Engineering, MIT, Cambridge, Massachusetts 02139.
[3] Nektonics, Cambridge, Massachusetts 02139.

854/5/4-1

is time, T is the final time of integration, $\underline{A}(t)$ and $\underline{B}(t)$ are general linear (or linearized) time-dependent operators, and $\underline{f}(t)$ is data. The operator $\underline{B}$ may be considered more generally to be related to a Lagrange multiplier, as described in Section 3. Although for our applications (1.1) represents a semidiscretization of a mixed initial-/boundary-value-problem partial differential equation, that is, $\underline{A}$ and $\underline{B}$ are matrices resulting from the discretization of spatial differential operators, the procedures proposed should be equally applicable to systems of ordinary differential equations.

It is often desirable to treat the $\underline{A}$ and $\underline{B}$ operators of (1.1) "separately." First, it may be the case that $\underline{A}$ and $\underline{B}$ are difficult to invert as the ensemble $\underline{A}+\underline{B}$, but are readily inverted independently. This occurs, for example, for $\underline{A}$ and $\underline{B}$ corresponding to the one-dimensional constituents of a multidimensional spatial operator (Douglas, 1955; Peaceman and Rachford, 1955); for fluid flow equations, with $\underline{A}$ representing the Coriolis force, a magnetic field, a Boussinesq temperature coupling, or (stiff) reaction kinetics (Bussing and Murman, 1988), and $\underline{B}$ representing the "classical" Navier–Stokes problem; for the incompressible Stokes problem, with $\underline{A}$ representing the divergence of the viscous stress tensor and $\underline{B}$ representing the pressure term and incompressibility constraint (Chorin, 1970; Temam, 1984; Orszag, Israeli, and Deville, 1986).

Second, even when the operators $\underline{A}$ and/or $\underline{B}$ are not readily inverted independently, splitting may still be advantageous if the $\underline{A}$ operator (say) is stiff relative to a computationally intensive $\underline{B}$ operator (Hofer, 1976; Gear, 1980); in this case, temporal decoupling is desirable in order to avoid unnecessary solution of the $\underline{B}$ system. Examples of this very common occurrence include: the system of ordinary differential equations describing the behavior of a collection of electronic devices, with $\underline{A}$ and $\underline{B}$ representing the "fast" and "slow" components/equations, respectively (White and Sangiovanni-Vincentelli, 1987; Saleh and Newton, 1989); the equations of reactor kinetics, with $\underline{A}$ representing the equations for prompt neutron density and $\underline{B}$ representing the equations for delayed neutron precursor density (Chao and Attard, 1985); a partial differential equation with a mesh spacing, and hence explicit time-step restriction, that is widely varying over the domain, with $\underline{A}$ representing the fine-mesh equations and $\underline{B}$ representing the coarse-mesh equations; the incompressible Navier–Stokes equations, with $\underline{A}$ representing the nonsymmetric, anisotropic convective terms (treated explicitly), and $\underline{B}$ representing the Stokes operator (treated implicitly) (Ewing and Russell, 1981; Pironneau, 1982; Benqué, Ibler, Keramsi, and Labadie, 1982; Gresho, Chan, Lee, and Upson, 1984).

In this article we introduce a new procedure, an "operator-integration-factor" method, which allows for the simple generation of high-order splitting techniques for equations of the general form given in (1.1). The outline

of the paper is as follows. In Sec. 2 we introduce the new approach and give several examples of schemes derived from the operator-integration-factor formalism. In Sec. 3 we apply these schemes to two problems arising in the simulation of incompressible flows, and give empirical evidence of the accuracy and efficiency of the methods. Lastly, in Sec. 4, we conclude with a brief description of outstanding questions that need to be resolved if operator-integration-factor methods are to be used with complete generality.

Notation. Unless otherwise indicated, we shall denote a matrix in $\mathscr{R}^{\mathscr{N}\times\mathscr{N}}$ as $\underline{A}$ (capital underscore), and a vector in $\mathscr{R}^{\mathscr{N}}$ as $\underline{u}$ (lower case underscore); on occasion we shall also write $\underline{u}=u_i=\{u_1,...,u_{\mathscr{N}}\}^T$, where superscript T denotes transpose. The inner product will be denoted $\underline{u}^T\underline{v}=\sum_{i=1}^{\mathscr{N}} u_i v_i$. Boldface vector notation, $\mathbf{u}=\{u_1,...,u_d\}^T$, will be reserved for vectors in physical space (e.g., $\mathscr{R}^d$ for $d=2$ or 3), with the associated dot product written as $\mathbf{u}\cdot\mathbf{v}=\sum_{i=1}^{d} u_i v_i$.

2. OPERATOR-INTEGRATION-FACTOR PROCEDURE

2.1. Operator Decoupling

To begin, we write (1.1) in terms of an integrating factor in $\underline{A}$,

$$\frac{d}{dt}\{\underline{Q}_{\underline{A}}^{(t^*;t)}\underline{u}(t)\}=\underline{Q}_{\underline{A}}^{(t^*;t)}[\underline{B}(t)\,\underline{u}+\underline{f}(t)] \tag{2.1}$$

in which t^* is an arbitrary fixed time. The integrating factor $\underline{Q}_{\underline{A}}^{(t^*;t)}$ is defined by the set of $\mathscr{N}^2$ differential equations,

$$\frac{d}{dt}\underline{Q}_{\underline{A}}^{(t^*;t)}=-\underline{Q}_{\underline{A}}^{(t^*;t)}\underline{A}(t) \tag{2.2}$$

$$\underline{Q}_{\underline{A}}^{(t^*;t^*)}=\underline{I} \tag{2.3}$$

where $\underline{I}$ is the identity operator. We remark that in the case where $\underline{A}(t_1)\,\underline{A}(t_2)=\underline{A}(t_2)\,\underline{A}(t_1)$ for any times t_1, t_2, such as when $\underline{A}$ is time independent or diagonal, $\underline{Q}_{\underline{A}}^{(t^*;t)}$ coincides with the exponential matrix, $\exp[\int_t^{t^*}\underline{A}(t')\,dt']$; for $\underline{A}(t)$ that do not commute, this scalar formula does not apply to the matrix case (Strang, 1990). Note it is assumed that all boundary conditions in space are *already* imposed on the discrete operators of (1.1), and thus (2.1) represents a restatement, not reformulation, of (1.1).

Integration of (2.1) requires the evaluation of integration-factor terms of the form

$$\underline{Q}_{\underline{A}}^{(t^*;t)}\underline{\psi}(t) \tag{2.4}$$

where $\underline{\psi}$ may be $\underline{u}$, $\underline{B}\underline{u}$, or $\underline{f}$. To avoid explicit construction of the $\underline{Q}$ matrix,

we introduce an auxiliary variable, $\tilde{\underline{\psi}}^{(t^*;t)}(s)$, and associated initial-value subproblem

$$\left(\frac{d\tilde{\underline{\psi}}^{(t^*;t)}}{ds}\right)(s) = \underline{A}(t+s)\,\tilde{\underline{\psi}}^{(t^*;t)}(s), \qquad 0 < s < (t^* - t) \tag{2.5}$$

$$\tilde{\underline{\psi}}^{(t^*;t)}(s=0) = \underline{\psi}(t) \tag{2.6}$$

from which we can then find

$$\underline{Q}_{\underline{A}}^{(t^*;t)}\underline{\psi}(t) = \tilde{\underline{\psi}}^{(t^*;t)}(t^* - t) \tag{2.7}$$

The final relation (2.7) follows from multiplying (2.5) by $\underline{Q}_{\underline{A}}^{(t^*;t+s)}$, and using (2.2), (2.3), and (2.6). $\underline{Q}$ may be thought of as the response matrix for the initial-value problem (2.5), and is also closely related to the Floquet matrix in the case where $\underline{A}(t)$ is time-periodic. In what follows we shall refer to Eqs. (2.5)–(2.7) as the associated-initial-value-problem process.

On the basis of Eqs. (2.1) and (2.5)–(2.7) the original coupled problem (1.1) can be broken into two effectively decoupled subproblems; (2.1) is integrated in the new variable

$$\underline{Q}_{\underline{A}}^{(t^*;t)}\underline{u}(t)$$

which is, in turn, evaluated from the associated initial-value problem (2.5)–(2.7). The particular numerical method generated by this operator-integration-factor approach is determined by the particular (finite-difference) time-stepping schemes chosen for (2.1) (scheme S_B) and (2.5) (scheme S_A); the resulting method will be denoted S_B/S_A. Note that the operator-integration-factor procedure is not a time-stepping scheme; rather, it is a procedure for the *generation* of time-stepping schemes. As a result, many of the methods generated by the operator-integration-factor approach are similar to known methods originally derived in a different fashion (see the references in the Introduction); other operator-integration-factor-derived schemes, however, appear to be new.

The use of integration factors in the numerical solution of partial differential equations, although not new (Rogallo, 1977; Spalart, 1986; Canuto, Hussaini, Quarteroni, and Zang, 1987), has been limited in the past primarily to diagonal operators, with no attempt at systematic operator decomposition. The use of integration factors in ordinary differential equations is more widespread, with application primarily to the splitting of coupled linear *time-independent* ($\underline{A}$)/nonlinear ($\underline{B}$) systems (Palusinski and Wait, 1978). These ordinary-differential-equation methods typically involve *explicit* construction of the matrix exponentials, (2.4), in a preprocessing stage of the computation. In contrast, in the method

proposed in the current paper, the integration-factor matrices are never formed; rather, we evaluate the *action* of the $\underline{\underline{Q}}$ matrices through solution of the associated initial-value problem, (2.5)–(2.7). The "action" approach offers advantages over the "explicit" exponentiation approach in generality (e.g., the treatment of time-dependent, and even nonlinear, $\underline{A}$), efficiency (e.g., the use of matrix-free evaluation of sparse operators), numerical stability, and simplicity. Recently proposed Krylov approximation methods (Freisner, Tuckerman, Dornblaser, and Russo) may improve the efficiency of the explicit exponentiation techniques for certain classes of problems.

In order to more clearly illustrate the basic concepts, we now turn to several examples of schemes derived from the operator-integration-factor approach.

2.2. Examples of Schemes

As described in the previous section, our operator-integration-factor approach involves discretization of (2.1) by a scheme S_B, and discretization of (2.5)–(2.7) by a scheme S_A. In the S_B discretization of (2.1) the approximation to $\underline{u}$ at time t^n will be denoted $\underline{u}^n = \underline{u}_{\Delta t}(t^n)$, where $t^n = n\Delta t$ and Δt is the time step. In the S_A discretization of (2.5) and (2.6) the approximation to $\underline{\tilde{\psi}}^{(t^*;t)}$ at "time" $s = m\Delta s$ will be denoted $\underline{\tilde{\psi}}^{(t^*;t)m} = \underline{\tilde{\psi}}^{(t^*;t)}_{\Delta s}(m\Delta s)$, where Δs is the "time step" within the subproblem (2.5) and (2.6). Note that temporal discretization of (2.5)–(2.7) is defined to comprise both the approximation of (2.5) *and* the replacement of $\underline{\tilde{\psi}}^{(t^*;t)}(s=0) = \underline{\psi}(t)$ by $\underline{\tilde{\psi}}^{(t^*;t)0} = \underline{\psi}_{\Delta t}(t)$ in (2.6). The resulting discrete approximation of (2.7) is denoted

$$S_A\{\underline{\underline{Q}}^{(t^*;t)}_{\underline{A}}\underline{\psi}_{\Delta t}(t)\} \equiv \underline{\tilde{\psi}}^{(t^*;t)(t^*-t)/\Delta s} \tag{2.8}$$

with Δs chosen such that $(t^*-t)/\Delta s$ is integer.

2.2.1. Euler Backward/Euler Backward

We take $t^* = t^{n+1}$ in (2.1) and apply the Euler-Backward scheme (S_B) (Gear, 1971) to the resulting equation to arrive at

$$\underline{u}^{n+1} - S_A\{\underline{\underline{Q}}^{(t^{n+1};t^n)}_{\underline{A}}\underline{u}^n\} = \Delta t[\underline{B}(t^{n+1})\underline{u}^{n+1} + \underline{f}^{n+1}] \tag{2.9}$$

where $\underline{f}^n = \underline{f}(t^n)$. Note that there is no "mixing" of operators on the right-hand side owing to the fact that the integration-factor term reduces to the identity operator for $t = t^{n+1}$; this is essential in achieving the desired decoupling of $\underline{A}$ and $\underline{B}$. To evaluate the exponential factor in (2.9) we apply

the associated-initial-value-problem process (2.5)–(2.7), discretizing (2.5) by the Euler-Backward scheme (S_A) with $\Delta s = \Delta t$,

$$\underline{\tilde{u}}^{(t^{n+1};t^n)1} - \underline{\tilde{u}}^{(t^{n+1};t^n)0} = \Delta s \underline{A}(t^{n+1})\, \underline{\tilde{u}}^{(t^{n+1};t^n)1} \tag{2.10}$$

$$\underline{\tilde{u}}^{(t^{n+1};t^n)0} = \underline{u}^n \tag{2.11}$$

$$S_A\{\underline{Q}_{\underline{A}}^{(t^{n+1};t^n)} u^n\} \equiv \underline{\tilde{u}}^{(t^{n+1};t^n)1} \tag{2.12}$$

Recall that the superscript $\cdot)\, m$ in $\underline{\tilde{u}}^{(t^{n+1};t^n)m}$ refers to the mth sub-time-step within the subproblem (2.5); here, $m = 0$ or 1 since $\Delta s = \Delta t$.

In order to more clearly demonstrate the decoupling effected by (2.9) and (2.10) we summarize the Euler-Backward/Euler-Backward scheme,

$$\underline{u}^{n+1} - \underline{\tilde{u}}^{(t^{n+1};t^n)1} = \Delta t[\underline{B}(t^{n+1})\, \underline{u}^{n+1} + \underline{f}^{n+1}] \tag{2.13}$$

$$\underline{\tilde{u}}^{(t^{n+1};t^n)1} - \underline{u}^n = \Delta t \underline{A}(t^{n+1})\, \underline{\tilde{u}}^{(t^{n+1};t^n)1} \tag{2.14}$$

Written in this form it is clear that the operator-integration-factor approach with Euler-Backward/Euler-Backward time differencing is, in fact, equivalent to the "standard" splitting approach proposed by numerous authors; the scheme is first order in time and unconditionally stable (assuming, for example, $\underline{u}^T \underline{A} \underline{u} < 0$, $\underline{u}^T \underline{B} \underline{u} < 0$).

2.2.2. *Crank–Nicolson/Crank–Nicolson*

We take $t^* = t^{n+1}$ in (2.1) and apply the Crank–Nicolson scheme (S_B) (Gear, 1971) to the resulting equation to arrive at

$$\underline{u}^{n+1} - S_A\{\underline{Q}_{\underline{A}}^{(t^{n+1};t^n)} \underline{u}^n\} = \frac{\Delta t}{2}\,[(\underline{B}(t^{n+1})\, \underline{u}^{n+1} + \underline{f}^{n+1}) + S_A\{\underline{Q}_{\underline{A}}^{(t^{n+1};t^n)} \underline{g}^n\}] \tag{2.15}$$

where for simplicity of notation we introduce $\underline{g}^n = \underline{B}(t^n)\, \underline{u}^n + \underline{f}^n$. To evaluate the two exponential factors in (2.15) we apply the associated-initial-value-problem process (2.5)–(2.7), discretizing (2.5) by the Crank–Nicolson scheme (S_A) with $\Delta s = \Delta t$. The resulting equations for the $\underline{u}^n$ and $\underline{g}^n$ integration factors are then

$$\underline{\tilde{u}}^{(t^{n+1};t^n)1} - \underline{\tilde{u}}^{(t^{n+1};t^n)0} = \frac{\Delta s}{2}\,[\underline{A}(t^{n+1})\, \underline{\tilde{u}}^{(t^{n+1};t^n)1} + \underline{A}(t^n)\, \underline{\tilde{u}}^{(t^{n+1};t^n)0}] \tag{2.16}$$

$$\underline{\tilde{u}}^{(t^{n+1};t^n)0} = \underline{u}^n \tag{2.17}$$

$$S_A\{\underline{Q}_{\underline{A}}^{(t^{n+1};t^n)} \underline{u}^n\} \equiv \underline{\tilde{u}}^{(t^{n+1};t^n)1} \tag{2.18}$$

and

$$\underline{\tilde{g}}^{(t^{n+1};t^n)1} - \underline{\tilde{g}}^{(t^{n+1};t^n)0} = \frac{\Delta s}{2}\left[\underline{A}(t^{n+1})\,\underline{\tilde{g}}^{(t^{n+1};t^n)1} + \underline{A}(t^n)\,\underline{\tilde{g}}^{(t^{n+1};t^n)0}\right] \quad (2.19)$$

$$\underline{\tilde{g}}^{(t^{n+1};t^n)0} = \underline{g}^n \quad (2.20)$$

$$S_A\{\underline{Q}_{\underline{A}}^{(t^{n+1};t^n)}\underline{g}^n\} \equiv \underline{\tilde{g}}^{(t^{n+1};t^n)1} \quad (2.21)$$

respectively.

We summarize the Crank–Nicolson/Crank–Nicolson scheme as

$$\underline{u}^{n+1} - \underline{\tilde{u}}^{(t^{n+1};t^n)1} = \frac{\Delta t}{2}\left[(\underline{B}(t^{n+1})\underline{u}^{n+1} + \underline{f}^{n+1}) + \underline{\tilde{g}}^{(t^{n+1};t^n)1}\right] \quad (2.22)$$

$$\underline{\tilde{u}}^{(t^{n+1};t^n)1} - \underline{u}^n = \frac{\Delta t}{2}\left[\underline{A}(t^{n+1})\,\underline{\tilde{u}}^{(t^{n+1};t^n)1} + \underline{A}(t^n)\,\underline{u}^n\right] \quad (2.23)$$

$$\underline{\tilde{g}}^{(t^{n+1};t^n)1} - \underline{g}^n = \frac{\Delta t}{2}\left[\underline{A}(t^{n+1})\,\underline{\tilde{g}}^{(t^{n+1};t^n)1} + \underline{A}(t^n)\,\underline{g}^n\right] \quad (2.24)$$

The resulting method is quite close to the classical second-order "method of approximate factorization" (Marchuk, 1971; Yanenko, 1971; Ames, 1977), albeit derived in a very different fashion. Note that replacement of $\underline{\tilde{g}}^{(t^{n+1};t^n)1}$ in (2.22) with g^n destroys the second-order accuracy of the method; we have verified this empirically (and accidentally) in the Stokes solver described in Sec. 3.1.3. As for the Euler-Backward/Euler-Backward scheme of the previous section, the Crank–Nicolson/Crank–Nicolson method completely decouples the inversion of $\underline{A}$ and $\underline{B}$, thereby permitting more effective solution methods to be pursued.

2.2.3. *Backward-Differentiation/Runge–Kutta*

We take $t^* = t^{n+1}$ in (2.1) and apply the Qth-order Backward-Differentiation scheme (S_B) (Gear, 1971) to the resulting equation to arrive at

$$\underline{u}^{n+1} - \sum_{q=1}^{Q} \beta_q S_A\{\underline{Q}_{\underline{A}}^{(t^{n+1};\,t^{n+1-q})}\underline{u}^{n+1-q}\} = \beta' \Delta t\left[\underline{B}(t^{n+1})\,\underline{u}^{n+1} + \underline{f}^{n+1}\right] \quad (2.25)$$

where the β_q, β' are the Backward-Differentiation coefficients (e.g., for $Q=3$, $\beta_1 = -18/11$, $\beta_2 = 9/11$, $\beta_3 = -2/11$, $\beta' = 6/11$). To evaluate the Q exponential factors in (2.25) we apply the associated-initial-value-problem process (2.5)–(2.7), discretizing (2.5) by the classical fourth-order explicit Runge–Kutta scheme (S_A) (Gear, 1971) with $\Delta s = \Delta t/M$ ($M \geqslant 1$ and integer): For $q = 1,\ldots, Q$,

$$
\begin{aligned}
\underline{g}_0 &= \underline{A}(t^{n+1-q} + m\,\Delta s)\,\tilde{\underline{u}}^{(t^{n+1};t^{n+1-q})m} \\
\underline{g}_1 &= \underline{A}(t^{n+1-q} + (m+1/2)\,\Delta s)\left(\tilde{\underline{u}}^{(t^{n+1};t^{n+1-q})m} + \frac{\Delta s}{2}\,\underline{g}_0\right) \\
\underline{g}_2 &= A(t^{n+1-q} + (m+1/2)\,\Delta s)\left(\tilde{\underline{u}}^{(t^{n+1};t^{n+1-q})m} + \frac{\Delta s}{2}\,\underline{g}_1\right) \\
\underline{g}_3 &= \underline{A}(t^{n+1-q} + (m+1)\,\Delta s)(\tilde{\underline{u}}^{(t^{n+1};t^{n+1-q})m} + \Delta s\underline{g}_2) \qquad (2.26) \\
\tilde{\underline{u}}^{(t^{n+1};t^{n+1-q})m+1} &= \tilde{\underline{u}}^{(t^{n+1};t^{n+1-q})m} + \frac{\Delta s}{6}(\underline{g}_0 + 2\underline{g}_1 + 2\underline{g}_2 + \underline{g}_3) \\
& \qquad m = 0,\ldots, qM-1
\end{aligned}
$$

with

$$
\tilde{\underline{u}}^{(t^{n+1};t^{n+1-q})0} = \underline{u}^{n+1-q} \qquad (2.27)
$$

and

$$
S_A\{\underline{Q}_{\underline{A}}^{(t^{n+1};t^{n+1-q})}\underline{u}^{n+1-q}\} \equiv \tilde{\underline{u}}^{(t^{n+1};t^{n+1-q})qM} \qquad (2.28)
$$

For convenience we have chosen Δs to be the same for all Q subproblems.

The complete Backward-Differentiation/Runga–Kutta scheme comprises (2.25) and (2.26)–(2.28). Unlike the Euler-Backward and Crank–Nicolson schemes of the previous subsections, the Backward-Differentiation/Runga–Kutta method admits no simple interpretation as a classical splitting scheme, and is, indeed, better described as a generalized, high-order subcycling approach (Gresho, Chan, Lee, and Upson, 1984). The method is formally order $\min(Q, 4)$ in time. Although there is no stability restriction on Δt in the implicit treatment of (2.25), stability of the explicit subproblem (2.26)–(2.28) requires $\Delta s \leqslant \Delta s_{\text{cr}}$, with Δs_{cr} determined (roughly) by the condition that the spectrum of $\Delta s\underline{A}$ lie within the absolute stability region of the explicit Runga–Kutta scheme.

The Backward-Differentiation/Runga–Kutta method is of interest in problems in which $\underline{A}$ is stiff, or difficult to invert, relative to a computationally intensive $\underline{B}$ system; this may occur, for example, when $\underline{B}$ represents a constraint, and therefore *must* be treated implicitly. To illustrate this point we consider, for purposes of comparison, solution of (1.1) [*not* (2.1)] by a standard semi-implicit scheme, with $\underline{A}$ treated by a modified third-order Adams–Bashforth technique (Gear, 1971; Ho, 1989), and $\underline{B}$ by the Qth-order Backward-Differentiation scheme. The critical time step for such a method is determined by the stability of the Adams–Bashforth method applied to $\underline{A}$, and will be denoted $\Delta t_{\text{cr,ref}}$. In the limit that *inversion* of the $\underline{B}$ system is infinitely more expensive than *evaluation* of the $\underline{A}$ operator, the Backward-Differentiation/Runge–Kutta scheme applied to (2.1) with time step Δt will be $\mathscr{S} = \sigma \equiv \Delta t/\Delta t_{\text{cr,ref}}$ faster than the Backward-Differentia-

tion/Adams–Bashforth method applied to (1.1); in practice, the actual speedup, $\mathscr{S}'$, will be slightly less, $\mathscr{S}' < \sigma$. (Note this analysis presumes that the time step in the standard semi-implicit approach is stability, not accuracy, limited.)

3. APPLICATION TO INCOMPRESSIBLE FLOW

We present here two examples of application of the methods developed in the previous section to important problems in the simulation of incompressible fluid flows: the first a velocity–pressure decoupling of the Stokes problem; the second a convection–Stokes decoupling of the Navier–Stokes equations.

3.1. A Full-Implicit Incompressible Stokes Method

3.1.1. Governing Equations

The equations governing the time-dependent incompressible flow of a highly viscous Newtonian fluid in a fixed domain Ω in $\mathscr{R}^d$ are the Stokes equations,

$$\frac{\partial \mathbf{u}}{\partial t} = \nabla^2 \mathbf{u} - \nabla p + \mathbf{f} \tag{3.1}$$

$$\nabla \cdot \mathbf{u} = 0 \tag{3.2}$$

with no-slip boundary conditions

$$\mathbf{u} = \mathbf{0} \tag{3.3}$$

applied on the domain boundary $\partial\Omega$. Here $\mathbf{u}(\mathbf{x}, t) = \{u_1, u_2, u_3\} = u_1(x, y, z, t)\,\mathbf{i} + u_2(x, y, z, t)\,\mathbf{j} + u_3(x, y, z, t)\,\mathbf{k}$ is the velocity, $p(x, y, z, t)$ is the pressure, and $\mathbf{f}(x, y, z, t)$ is an applied force. The density of the fluid is taken to be unity, and the viscosity is folded into time and the pressure.

We next consider a variational (e.g., finite element) discretization of (3.1)–(3.3). In particular, we construct a semidiscrete (in space) approximation to $(\mathbf{u}, p) \in (X, Y)$, $(\mathbf{u}_h, p_h) \in (X_h, Y_h)$. Here (X, Y) are the spaces in which the variational formulation of (3.7)–(3.3) is well posed, and $X_h \subset X$, $Y_h \subset Y$ are appropriate conforming approximation subspaces (Girault and Raviart, 1986). We then choose a basis for $(\mathbf{u}_h, p_h)$, writing $\mathbf{u}_h(\mathbf{x}, t) = \underline{\mathbf{u}}_h^T(t)\,\underline{\vartheta}_h(\mathbf{x})$, $p_h(\mathbf{x}, t) = \underline{p}_h^T(t)\,\underline{\varphi}_h(\mathbf{x})$; for example, a nodal basis satisfies $\vartheta_{hi}(\mathbf{x}_{hj}) = \delta_{ij}$, where $\underline{\mathbf{x}}_h$ is some unisolvent set of basis points, and δ_{ij} is the Kronecker delta symbol. The discrete equations for the basis coefficients $(\underline{\mathbf{u}}_h, \underline{p}_h) \in ((\mathscr{R}^{\mathscr{N}})^d, \mathscr{R}^{\mathscr{M}})$ are then given by

$$\underline{M}_h \frac{d\underline{\mathbf{u}}_h}{dt} = -\underline{L}_h \underline{\mathbf{u}}_h + \underline{\mathbf{D}}_h^T \underline{p}_h + \underline{M}_h \underline{\mathbf{f}}_h \tag{3.4}$$

$$\underline{\mathbf{D}}_h \cdot \underline{\mathbf{u}}_h = 0 \tag{3.5}$$

where $\underline{M}_h \in \mathrm{R}^{\mathcal{N} \times \mathcal{N}}$, $\underline{L}_h \in \mathscr{R}^{\mathcal{N} \times \mathcal{N}}$, and $\underline{\mathbf{D}}_h \in (\mathscr{R}^{\mathcal{M} \times \mathcal{N}})^d$ are, respectively, the basis-specific mass, $-\nabla^2$, and gradient matrices derived from the corresponding bilinear forms in the variational formulation of (3.1)–(3.3). The vector $\underline{\mathbf{f}}_h$ contains the $\mathcal{J}_h$ basis coefficients of an appropriate projection or interpolation of the continuous force $\mathbf{f}$. We assume that all essential boundary conditions (3.3) are implicitly represented in (3.4) and (3.5) through elimination of appropriate basis coefficients. In essence, (3.4), (3.5) can now be considered as a system of ordinary differential equations, amenable to classical "method-of-lines" discretization in time.

Complete numerical resolution of (3.4), (3.5) requires two further steps: choice of a time-stepping scheme; and choice of an inversion procedure for the resulting implicit equations (we consider only implicit methods given the relatively severe stability restrictions associated with the Laplacian operator). A common approach to this discretization/solution problem comprises: a standard full-implicit time-stepping procedure, such as Euler-Backward, Crank–Nicolson, or Backward-Differentiation; Uzawa transformation of the resulting fully discrete system to $d+1$ "uncoupled" elliptic equations (Arrow, Hurwicz, and Uzawa, 1958; Glowinski, 1984; Temam, 1984; Girault and Raviart, 1986; Cahouet and Chabard, 1986; Maday, Patera, and Rønquist, 1987; Bristeau, Glowinski, and Periaux; Maday, Meiron, Patera, and Rønquist); solution of the elliptic equations by iterative procedures such as the conjugate gradient method (Golub and van Loan, 1983). This approach, though viable, suffers from the fact that the Uzawa pressure equation involves an inverse Laplacian, and therefore must be solved as a *nested* elliptic iteration.

It is clear that a time-splitting approach to (3.4), (3.5) that would reduce the resulting implicit equations to more tractable (e.g., truly decoupled, that is, non-nested) form while simultaneously maintaining high-order accuracy is highly desirable. In the two subsections that follow we propose two such methods based on the Euler-Backward/Euler-Backward and Crank–Nicolson/Crank–Nicolson schemes presented in Sec. 2.

Remark 1. The time-stepping procedures developed in the current article should be applicable to a wide range of variational (and non-variational) spatial discretizations. For purposes of numerical example, however, we shall focus primarily on one particular variational spatial treatment, the Legendre "$\mathbf{P}_N \times \mathbf{P}_{N-2}$" spectral element Stokes and Navier–Stokes discretization (Maday, Patera, and Rønquist, 1987; Rønquist, 1988; Maday and Patera, 1989). Spectral element discretizations

are especially appropriate candidates for time-splitting approaches given the rapid growth of the extreme eigenvalues of spectral operators (Weideman and Trefethen; Vandeven, 1990); *high-order* time-splitting methods are of particular interest in the spectral context given the rapid convergence rate of spectral methods in space (Canuto, Hussaini, Quarteroni, and Zang, 1987).

Remark 2. We note that although splitting approaches have not, to our knowledge, been applied to (3.4), (3.5), they have been vigorously pursued in the context of the pressure-Poisson form of the Stokes problem (Chorin, 1971; Temam, 1984; Kim and Moin, 1985; Orszag, Israeli, and Deville, 1986; Zang and Hussaini, 1986; Karniadakis, Israeli, and Orszag, 1990). In many cases the divergence form of the Stokes problem, (3.4), (3.5), is preferred over the Poisson form of the equations, in that the former, unlike the latter, makes no assumptions as regards boundary conditions or the form of the stress tensor; in particular, the divergence representation can readily treat free surface flows (Ho and Patera, 1990a; Ho and Patera, 1990b), and flows involving variable viscosity or complex rheology. The divergence form of the equations also offers a better theoretical framework, especially as regards the analysis of spatial discretization errors. For these reasons we believe that the success of splitting methods for the Poisson formulation does not mitigate the need for corresponding progress in the divergence approach.

3.1.2. Euler-Backward/Euler-Backward

We apply the Euler-Backward/Euler-Backward method of Sec. 2.2.1 to (3.4), (3.5), with $\underline{A}$ associated with $-\underline{L}_h$, and $\underline{B}$ associated with the pressure/divergence "$\underline{\mathbf{D}}_h$ system." The resulting method can be written, analogously to (2.13), (2.14), as

$$\underline{M}_h \underline{\mathbf{u}}_h^{n+1} - \underline{M}_h \tilde{\underline{\mathbf{u}}}_h^{(t^{n+1};t^n)1} = \Delta t[\underline{\mathbf{D}}_h^T \underline{p}_h^{n+1} + \underline{M}_h \underline{\mathbf{f}}_h^{n+1}] \tag{3.6}$$

$$\underline{\mathbf{D}}_h \cdot \underline{\mathbf{u}}_h^{n+1} = 0 \tag{3.7}$$

$$\underline{M}_h \tilde{\underline{\mathbf{u}}}_h^{(t^{n+1};t^n)1} - \underline{M}_h \underline{\mathbf{u}}_h^n = -\Delta t \underline{L}_h \tilde{\underline{\mathbf{u}}}_h^{(t^{n+1};t^n)1} \tag{3.8}$$

where $\underline{\mathbf{u}}_h^n = \underline{\mathbf{u}}_{h,\Delta t}(t^n)$. Note that $\underline{M}_h$, $\underline{L}_h$, and $\underline{\mathbf{D}}_h$ are not functions of time, and thus time-level superscripts are omitted. We next apply a "Uzawa" procedure to (3.6), (3.7), arriving at the final set of equations

$$\underline{M}_h \underline{\mathbf{u}}_h^{n+1} - \underline{M}_h \tilde{\underline{\mathbf{u}}}_h^{(t^{n+1};t^n)1} = \Delta t[\underline{\mathbf{D}}_h^T \underline{p}_h^{n+1} + \underline{M}_h \underline{\mathbf{f}}_h^{n+1}] \tag{3.9}$$

$$-\underline{\mathbf{D}}_h \cdot \underline{M}_h^{-1} \underline{\mathbf{D}}_h^T \underline{p}_h^{n+1} = \underline{\mathbf{D}}_h \cdot (\tilde{\underline{\mathbf{u}}}_h^{(t^{n+1};t^n)1}/\Delta t + \underline{\mathbf{f}}_h^{n+1}) \tag{3.10}$$

$$\underline{M}_h \tilde{\underline{\mathbf{u}}}_h^{(t^{n+1};t^n)1} - \underline{M}_h \underline{\mathbf{u}}_h^n = -\Delta t \underline{L}_h \tilde{\underline{\mathbf{u}}}_h^{(t^{n+1};t^n)1} \tag{3.11}$$

which must be solved at each time step. Note that (3.6)–(3.8) and (3.9)–(3.11) are discretely equivalent.

These equations are completely decoupled, requiring d elliptic solves in (3.11), and one elliptic solve in (3.10). Although the elliptic operator in (3.10) may appear nested, the spectral element mass matrix is, in fact, diagonal, and thus $\underline{M}_h^{-1}$ requires no iteration. (Finite element mass matrices would need to be "lumped" to avoid nested elliptic solves.) We note that the operator $\underline{E}_h = -\underline{\mathbf{D}}_h \cdot \underline{M}_h^{-1} \underline{\mathbf{D}}_h^T$ in (3.10) plays the role of a Laplacian; $\underline{E}_h$ is, in fact, a "complementary mixed" formulation of the Laplacian which is, unfortunately, less readily preconditioned than the standard variational form.

Remark 3. If we were to apply the standard *(unsplit)* Euler backward method to (3.4), (3.5), and then apply the Uzawa procedure, the resulting discrete pressure operator would be $\underline{S}_h = -\underline{\mathbf{D}}_h \cdot \underline{H}_h^{-1} \underline{\mathbf{D}}_h^T$, where $\underline{H}_h = \underline{L}_h + (1/\Delta t)\, \underline{M}_h$ is the discrete Helmholtz operator. Hence, iterative inversion of $\underline{S}_h$ requires d elliptic (Helmholtz) solves for each pressure iteration, that is, the iteration involves nested elliptic solves. Nested iteration is eliminated by the splitting methods described in this paper.

3.1.3. *Crank–Nicolson/Crank–Nicolson*

We apply the Crank–Nicolson/Crank–Nicolson method of Sec. 2.2.2 to (3.4), (3.5), with $\underline{A}$ associated with $-\underline{L}_h$, and $\underline{B}$ associated with the pressure/divergence "$\underline{\mathbf{D}}_h$ system." The resulting method can be written, analogously to (2.22)–(2.24), as

$$\underline{M}_h \underline{\mathbf{u}}_h^{n+1} - \underline{M}_h \tilde{\underline{\mathbf{u}}}_h^{(t^{n+1};\, t^n)1} = \frac{\Delta t}{2} \left[(\underline{\mathbf{D}}_h^T \underline{p}_h^{n+1} + \underline{M}_h \underline{\mathbf{f}}_h^{n+1}) + \underline{M}_h \tilde{\underline{\mathbf{g}}}_h^{(t^{n+1};\, t^n)1} \right] \tag{3.12}$$

$$\underline{\mathbf{D}}_h \cdot \underline{\mathbf{u}}_h^{n+1} = 0 \tag{3.13}$$

$$\underline{M}_h \tilde{\underline{\mathbf{u}}}_h^{(t^{n+1};\, t^n)1} - \underline{M}_h \underline{\mathbf{u}}_h^n = -\frac{\Delta t}{2} \left[\underline{L}_h \tilde{\underline{\mathbf{u}}}_h^{(t^{n+1};\, t^n)1} + \underline{L}_h \underline{\mathbf{u}}_h^n \right] \tag{3.14}$$

$$\underline{M}_h \tilde{\underline{\mathbf{g}}}_h^{(t^{n+1};\, t^n)1} - \underline{M}_h \underline{\mathbf{g}}_h^n = -\frac{\Delta t}{2} \left[\underline{L}_h \tilde{\underline{\mathbf{g}}}_h^{(t^{n+1};\, t^n)1} + \underline{L}_h \underline{\mathbf{g}}_h^n \right] \tag{3.15}$$

where $\underline{\mathbf{g}}_h^n = \underline{M}_h^{-1} \underline{\mathbf{D}}_h^T \underline{p}_h^n + \underline{\mathbf{f}}_h^n$. We then apply a Uzawa procedure to obtain

$$\underline{M}_h \underline{\mathbf{u}}_h^{n+1} - \underline{M}_h \tilde{\underline{\mathbf{u}}}_h^{(t^{n+1};\, t^n)1} = \frac{\Delta t}{2} \left[(\underline{\mathbf{D}}_h^T \underline{p}_h^{n+1} + \underline{M}_h \underline{\mathbf{f}}_h^{n+1}) + \underline{M}_h \tilde{\underline{\mathbf{g}}}_h^{(t^{n+1};\, t^n)1} \right] \tag{3.16}$$

$$-\underline{\mathbf{D}}_h \cdot \underline{M}_h^{-1} \underline{\mathbf{D}}_h^T \underline{p}_h^{n+1} = \underline{\mathbf{D}}_h \cdot (2\tilde{\underline{\mathbf{u}}}_h^{(t^{n+1};\, t^n)1}/\Delta t + \underline{\mathbf{f}}_h^{n+1} + \tilde{\underline{\mathbf{g}}}_h^{(t^{n+1};\, t^n)1}) \tag{3.17}$$

$$\underline{M}_h \tilde{\underline{\mathbf{u}}}_h^{(t^{n+1};t^n)1} - \underline{M}_h \underline{\mathbf{u}}_h^n = -\frac{\Delta t}{2}\left[\underline{L}_h \tilde{\underline{\mathbf{u}}}_h^{(t^{n+1};t^n)1} + \underline{L}_h \underline{\mathbf{u}}_h^n\right] \tag{3.18}$$

$$\underline{M}_h \tilde{\underline{\mathbf{g}}}_h^{(t^{n+1};t^n)1} - \underline{M}_h \underline{\mathbf{g}}_h^n = -\frac{\Delta t}{2}\left[\underline{L}_h \tilde{\underline{\mathbf{g}}}_h^{(t^{n+1};t^n)1} + \underline{L}_h \underline{\mathbf{g}}_h^n\right] \tag{3.19}$$

which must be solved at each time step. The computational procedure and complexity are the same as for the Euler-Backward scheme (3.9)–(3.11), save for the additional elliptic solve, (3.19).

It is of interest in the case of this Crank–Nicolson scheme to note that (3.16)–(3.19) is equivalent to

$$\begin{aligned}\underline{M}_h\left(\frac{\underline{\mathbf{u}}_h^{n+1} - \underline{\mathbf{u}}_h^n}{\Delta t}\right) &= -\frac{1}{2}\underline{L}_h(\underline{\mathbf{u}}_h^{n+1} + \underline{\mathbf{u}}_h^n) + \frac{1}{2}\left[(\underline{\mathbf{D}}_h^T \underline{p}_h^{n+1} + \underline{M}_h \underline{\mathbf{f}}_h^{n+1}) + (\underline{\mathbf{D}}_h^T \underline{p}_h^n + \underline{M}_h \underline{\mathbf{f}}_h^n)\right] \\ &\quad + \frac{\Delta t^2}{4}\underline{L}_h\left[\frac{\left[(\underline{M}_h^{-1}\underline{\mathbf{D}}_h^T \underline{p}_h^{n+1} + \underline{\mathbf{f}}_h^{n+1}) - (\underline{M}_h^{-1}\underline{\mathbf{D}}_h^T \underline{p}_h^n + \underline{\mathbf{f}}_h^n)\right]}{\Delta t}\right]\end{aligned} \tag{3.20}$$

$$\underline{\mathbf{D}}_h \cdot \underline{\mathbf{u}}_h^{n+1} = 0 \tag{3.21}$$

It is seen that the method corresponds to an "unsplit" Crank–Nicolson scheme augmented by an additional term which is formally $O(\Delta t^2)$; indeed, (3.20) has the form typical of splitting approximations. The value of the operator-integration-factor approach is in providing a systematic procedure by which to generate consistent approximations which, by construction, admit decoupling of the constituent operators. Note that at steady state all splitting errors vanish in (3.20); this does not, of course, imply that arbitrarily large time steps should be taken, given the behavior of the Crank–Nicolson scheme for large Δt.

3.1.4. Numerical Results

We consider here the two-dimensional model problem analyzed in detail by Deville, Kleiser, and Montigny (1984), and Orszag, Israeli, and Deville (1986). The governing equations (3.1), (3.2) are solved in a domain Ω defined by $0 \leqslant x \leqslant 2\pi$, $-1 < y < 1$. The velocity $\mathbf{u} = u_1(x, y, t)\,\mathbf{i} + u_2(x, y, t)\,\mathbf{j}$ is required to be 2π-periodic in x, and to satisfy no-slip boundary conditions, (3.3), in y, $u_1(x, \pm 1, t) = u_2(x, \pm 1, t) = 0$. The initial conditions are taken to be the least-stable eigenfunction of the Stokes operator,

$$u_{1\,0}(x, y) = \sin x(a \cosh k \sin ay - \cos a \sinh y) \tag{3.22}$$

$$u_{2\,0}(x, y) = \cos x(\cosh k \cos ay - \cos a \cosh y) \tag{3.23}$$

where $a \approx 2.883356$, for which the exact solution is then

$$u_1(x, y, t) = \sin x(a \cosh k \sin ay - \cos a \sinh y)\, e^{-\lambda t} \tag{3.24}$$

$$u_2(x, y, t) = \cos x(\cosh k \cos ay - \cos a \cosh y)\, e^{-\lambda t} \tag{3.25}$$

$$p(x, y, t) = -\lambda(\cos a \cos x \sinh y)\, e^{-\lambda t} \tag{3.26}$$

with eigenvalue $\lambda \approx 9.313739$.

Our numerical tests are for the case of the Legendre "$\mathbf{P}_N \times \mathbf{P}_{N-2}$" spectral element Stokes discretization (Maday, Patera, and Rønquist, 1987;

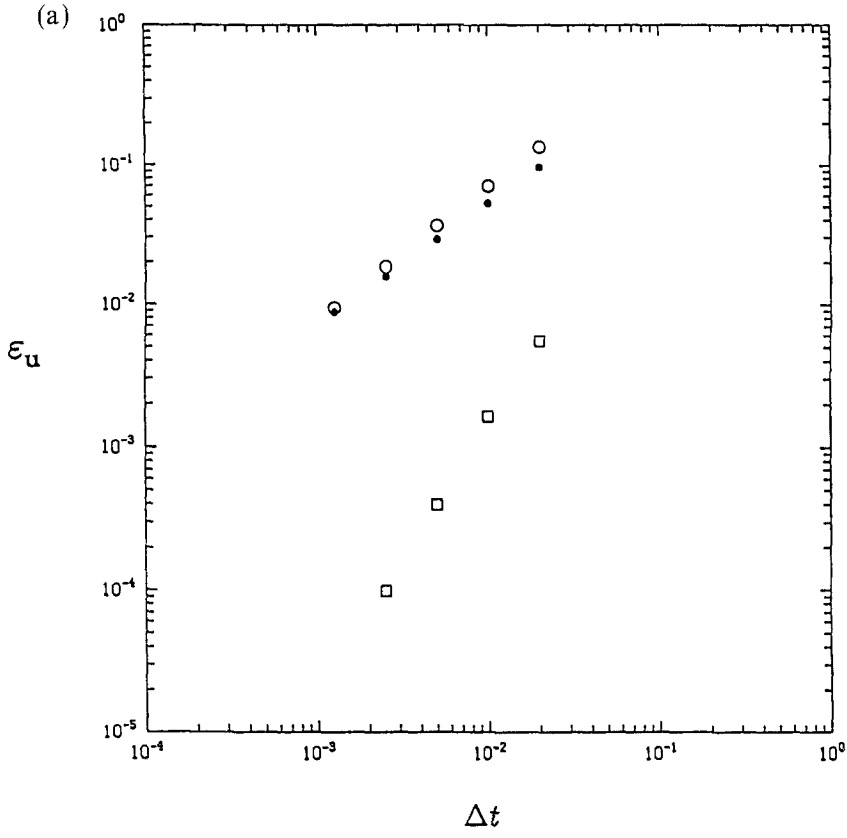

Fig. 1. In (a) we plot the velocity error measured in the relative H^1-norm, ε_u, at time $T = 0.1$ as a function of the time step Δt for solution of the two-dimensional, unsteady Stokes problem (3.1), (3.2) subject to initial conditions given by (3.22), (3.23). In (b) the corresponding pressure error measured in the relative L^2-norm, ε_p, is shown. The results are obtained using the Euler backward/Euler backward method (3.6)–(3.11) (○) and the Crank–Nicolson/ Crank–Nicolson method (3.12)–(3.19) (□). For comparison we also show the results using the classical first-order Stokes-splitting scheme (●).

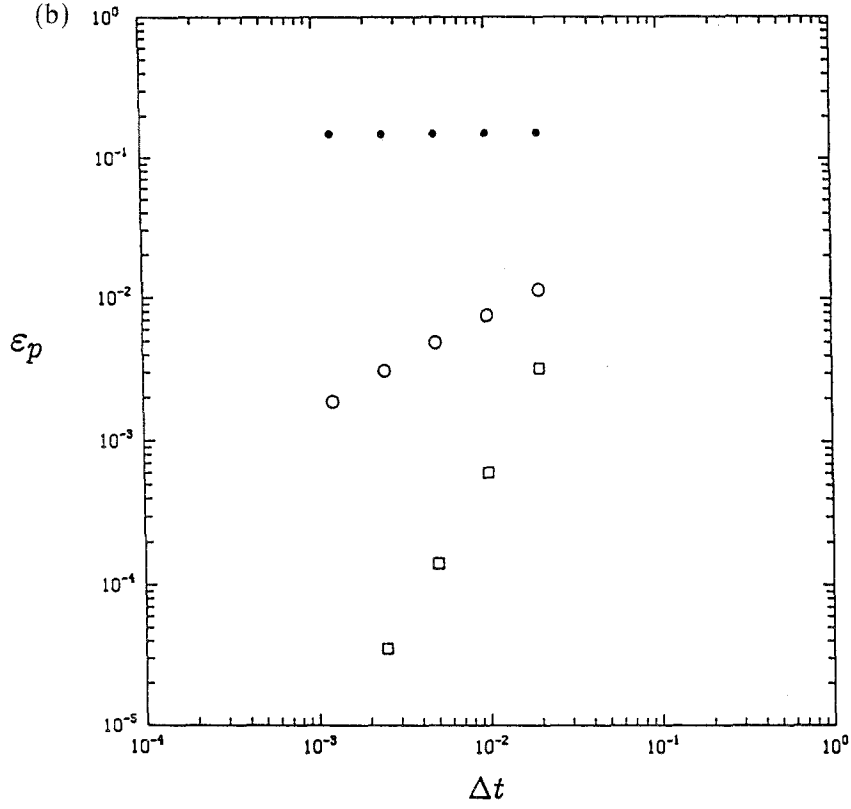

Fig. 1. Continued.

Rønquist, 1988; Maday and Patera, 1989) using $K=6$ elements, each of polynomial order N in each of the two spatial directions. In all cases the discrete equations are integrated to a final time $T=0.1$, at which time the solution has decayed to roughly 1/3 of its initial amplitude. The velocity error, $\varepsilon_{\mathbf{u}}$, is measured at time T in the (relative) H^1-norm (Adams, 1975) in space $[\sum_{i=1}^{d=2} \|u_i(\cdot, T) - u_{h,\Delta t i}(\cdot, T)\|_{H^1}^2]^{1/2} / [\sum_{i=1}^{d=2} \|u_i(\cdot, T)\|_{H^1}^2]^{1/2}$; the pressure error, ε_p, is measured at time T in the (relative) L^2 norm, $\|p(\cdot, T) - p_{h,\Delta t}(\cdot, T)\|_{L^2} / \|p(\cdot, T)\|_{L^2}$. Spatial convergence is examined by considering the dependence of $\varepsilon_{\mathbf{u}}$ and ε_p on N for sufficiently small Δt; temporal convergence is examined by considering the dependence of $\varepsilon_{\mathbf{u}}$ and ε_p on Δt for sufficiently large N.

We begin by examining the temporal error by plotting in Figs. 1a and 1b the velocity and pressure errors, respectively, as a function of Δt for the Euler-Backward and Crank–Nicolson Stokes schemes of Secs. 3.1.2 and 3.1.3. We take a polynomial order of $N=8$ in each element, which is suf-

ficient to ensure that there is effectively no spatial contribution to the error. It is seen that, consistent with our formal expectations, the Euler-Backward and Crank–Nicolson schemes are first- and second-order accurate in time, respectively, in both the velocity *and* the pressure. The very significant advantage of greater than first-order methods is clearly demonstrated by the large reduction in error of the Crank–Nicolson scheme relative to the Euler-Backward method. Note that at $\Delta t = 0.01$ the error in the Crank–Nicolson scheme is 1.65×10^{-3}; this time step is roughly .1 the time scale of the eigenfunction decay $(1/\lambda)$, and roughly 10 times the critical time step that would result were an explicit scheme used for the viscous terms. By virtue of elimination of nested iterations, both the Euler-Backward and Crank–Nicolson methods promise to be faster than corresponding standard Uzawa Stokes-decoupling procedures; however, we have not yet performed a fair comparison between the two approaches.

We have also plotted in Figs. 1a and 1b the velocity and pressure errors obtained using a Legendre "$\mathbf{P}_N \times \mathbf{P}_N$" spectral element approximation (Karniadakis) of the classical first-order Stokes splitting scheme based on a pressure-Poisson equation with invisicid Neumann boundary conditions (Chorin, 1970; Temam, 1984; Orszag, Israeli, and Deville, 1986). Although the error in the velocity is, first order, the pressure converges much more slowly owing to the incorrect (inviscid) boundary condition. This poor convergence is by no means a general indictment of the Poisson approach, for which numerous high-order extensions have been proposed (Kim and Moin, 1985; Orszag, Israeli, and Deville, 1986; Zang and Hussaini, 1986; Karniadakis, Israeli, and Orszag); it does, however, indicate the tendency of the divergence form of the equations to produce more uniformly convergent schemes in time and space. In fairness to the Poisson schemes it should be noted that the divergence-form uniformity comes at some cost. Although the new schemes proposed in this article and the pressure-Poisson approaches both require the same number of elliptic solves per time step $(d+1)$, the latter involve only "standard" Laplacian discretizations, whereas the former also generate the more problematic $\underline{E}_h$ system described in Sec. 3.1.2.

Lastly, as regards spatial convergence, we have verified that the Euler-Backward and Crank–Nicolson schemes converge to the exact solution exponentially fast in N for sufficiently small Δt, as would be expected for a spectral approximation to an infinitely smooth solution. In contrast, whereas the first-order pressure-Poisson approach does achieve spectral accuracy in the velocity, it cannot achieve spectral accuracy in the pressure without postprocessing owing to the incorrect (inviscid) boundary condition. Higher-order methods in the Poisson context improve the pressure convergence significantly.

3.2. A Lagrangian/Subcycling Method for the Incompressible Navier–Stokes Equations

3.2.1. Governing Equations

We consider here the full incompressible Navier–Stokes equations (Temam, 1984; Girault and Raviart, 1986) governing the time-dependent flow of a viscous Newtonian fluid in a fixed domain Ω in $\mathscr{R}^d$,

$$\frac{\partial \mathbf{u}}{\partial t} = -\mathbf{u}\cdot\nabla\mathbf{u} + \nu\nabla^2\mathbf{u} - \nabla(p/\rho) + \mathbf{f} \tag{3.27}$$

$$\nabla\cdot\mathbf{u} = 0 \tag{3.28}$$

with no-slip boundary conditions

$$\mathbf{u} = \mathbf{0} \tag{3.29}$$

applied on the domain boundary $\partial\Omega$. The density and kinematic viscosity of the fluid are denoted ρ and ν, respectively. As for the Stokes problem, we consider the semidiscrete (in space) approximation $(\mathbf{u}_h, p_h)$ to $(\mathbf{u}, p)$ obtained from a variational discretization (Girault and Raviart, 1986) of (3.27)–(3.29),

$$\underline{M}_h \frac{d\underline{\mathbf{u}}_h}{dt} = -\underline{C}_h(\underline{\mathbf{u}}_h)\underline{\mathbf{u}}_h - \nu\underline{L}_h\underline{\mathbf{u}}_h + \underline{\mathbf{D}}_h^T(\underline{p}_h/\rho) + \underline{M}_h\underline{\mathbf{f}}_h \tag{3.30}$$

$$\underline{\mathbf{D}}_h\cdot\underline{\mathbf{u}}_h = 0 \tag{3.31}$$

with $\underline{M}_h$, $\underline{L}_h$, $\underline{\mathbf{D}}_h$, and $\underline{\mathbf{f}}_h$ defined as for (3.4), (3.5). The convection matrix, $\underline{C}_h(\underline{\mathbf{u}}_h) \in \mathscr{R}^{\mathscr{N}\times\mathscr{N}}$, represents the discrete form of $\mathbf{u}\cdot\nabla$, which can be written in convective, conservative, or skew-symmetric form.

3.2.2. Backward-Differentiation/Runge–Kutta Method

We apply the Backward-Differentiation/Runge–Kutta method of Sec. 2.2.3 to (3.30), (3.31), with $\underline{A}$ associated with $-\underline{C}_h$, and $\underline{B}$ associated with the full Stokes operator. The resulting method can be written, following (2.25), as

$$\underline{M}_h\left[\underline{\mathbf{u}}_h^{n+1} - \sum_{q=1}^{Q}\beta_q S_A\{\underline{Q}^{(t^{n+1};t^{n+1-q})}_{\underline{M}_h^{-1}\underline{C}_h(\underline{\mathbf{U}}_h^{n+1}(\cdot))}\underline{\mathbf{u}}_h^{n+1-q}\}\right]$$
$$= \beta'\Delta t[-\nu\underline{L}_h\underline{\mathbf{u}}_h^{n+1} + \underline{\mathbf{D}}_h^T(\underline{p}_h^{n+1}/\rho) + \underline{M}_h\underline{\mathbf{f}}_h^{n+1}] \tag{3.32}$$

$$\underline{\mathbf{D}}_h\cdot\underline{\mathbf{u}}_h^{n+1} = 0 \tag{3.33}$$

where $\underline{\mathbf{u}}_h^n = \underline{\mathbf{u}}_{h,\Delta t}(t^n)$, and the β_q, β' are defined in Sec. 2.2.3. Here $\underline{\mathbf{U}}_h^{n+1}(t)$ is the $(Q-1)$th-order polynomial extrapolant of the discrete velocity on the time interval $(t^{n+1} - Q\Delta t) \leqslant t \leqslant t^{n+1}$ based on $\underline{\mathbf{u}}_h^n, \ldots, \underline{\mathbf{u}}_h^{n+1-Q}$; for example, for $Q=1$, $\underline{\mathbf{U}}_h^{n+1}(t) = \underline{\mathbf{u}}_h^n$ (Maday, Patera, and Rønquist). Following (2.26)–(2.28), we then solve

For $q = 1, \ldots, Q$,

$$\underline{M}_h \underline{\mathbf{g}}_0 = -\underline{C}_h(\underline{\mathbf{U}}_h^{n+1}(t^{n+1-q} + m\,\Delta s))\,\tilde{\underline{\mathbf{u}}}_h^{(t^{n+1};\,t^{n+1-q})m}$$

$$\underline{M}_h \underline{\mathbf{g}}_1 = -\underline{C}_h(\underline{\mathbf{U}}_h^{n+1}(t^{n+1-q} + [m+1/2]\,\Delta s))\left(\tilde{\underline{\mathbf{u}}}_h^{(t^{n+1};\,t^{n+1-q})m} + \frac{\Delta s}{2}\,\underline{\mathbf{g}}_0\right)$$

$$\underline{M}_h \underline{\mathbf{g}}_2 = -\underline{C}_h(\underline{\mathbf{U}}_h^{n+1}(t^{n+1-q} + [m+1/2]\,\Delta s))\left(\tilde{\underline{\mathbf{u}}}_h^{(t^{n+1};\,t^{n+1-q})m} + \frac{\Delta s}{2}\,\underline{\mathbf{g}}_1\right)$$

$$\underline{M}_h \underline{\mathbf{g}}_3 = -\underline{C}_h(\underline{\mathbf{U}}_h^{n+1}(t^{n+1-q} + [m+1]\,\Delta s))(\tilde{\underline{\mathbf{u}}}_h^{(t^{n+1};\,t^{n+1-q})m} + \Delta s\,\underline{\mathbf{g}}_2)$$

$$\tilde{\underline{\mathbf{u}}}_h^{(t^{n+1};\,t^{n+1-q})m+1} = \tilde{\underline{\mathbf{u}}}_h^{(t^{n+1};\,t^{n+1-q})m} + \frac{\Delta s}{6}(\underline{\mathbf{g}}_0 + 2\underline{\mathbf{g}}_1 + 2\underline{\mathbf{g}}_2 + \underline{\mathbf{g}}_3), \qquad (3.34)$$

$$m = 0, \ldots, qM - 1$$

with

$$\tilde{\underline{\mathbf{u}}}_h^{(t^{n+1};\,t^{n+1-q})0} = \underline{\mathbf{u}}_h^{n+1-q} \qquad (3.35)$$

and

$$S_A\{\underline{\mathcal{Q}}_{-\underline{M}_h^{-1}\underline{C}_h(\underline{\mathbf{U}}_h^{n+1}(\cdot))}^{(t^{n+1};\,t^{n+1-q})}\underline{\mathbf{u}}_h^{n+1-q}\} \equiv \tilde{\underline{\mathbf{u}}}_h^{(t^{n+1};\,t^{n+1-q})qM} \qquad (3.36)$$

Effective linearization is critical to the success of the integration-factor approach.

We remark that examination of the left-hand side of (3.32) suggests that, by virtue of the integration-factor decomposition, we have replaced the *sum* of the unsteady and convection terms in (3.30) with a single substantial derivative. To see this more readily, we consider the initial-value problem (2.5)–(2.7) associated with the $q=1$ integration factor of (3.32) prior to spatial and temporal discretization,

$$\frac{d\tilde{\mathbf{u}}^{(t^{n+1};\,t^n)}(s)}{ds} = -\mathbf{u}(\mathbf{x},\, t^n + s)\cdot\nabla\tilde{\mathbf{u}}^{(t^{n+1};\,t^n)}(s), \qquad 0 < s < \Delta t \quad (3.37)$$

$$\tilde{\mathbf{u}}^{(t^{n+1};\,t^n)}(\mathbf{x},\, s=0) = \mathbf{u}(\mathbf{x},\, t^n) \qquad (3.38)$$

$$\mathcal{Q}_{-\mathbf{u}(\mathbf{x},\,\cdot)\nabla}^{(t^{n+1};\,t^n)}\mathbf{u}(\mathbf{x},\, t^n) = \tilde{\mathbf{u}}^{(t^{n+1};\,t^n)}(\mathbf{x},\, s=\Delta t) \qquad (3.39)$$

It follows from the solution of (3.37), (3.38) that (3.39) can also be written as

$$Q^{(t^{n+1};\,t^n)}_{-\mathbf{u}(\mathbf{x},\,\cdot)\nabla}\mathbf{u}(\mathbf{x},\,t^n) = \mathbf{u}\left(\mathbf{x} - \int_{t^n}^{t^{n+1}} \mathbf{u}(\mathbf{X}(\mathbf{x},\,t'),\,t')\,dt',\,t^n\right) \tag{3.40}$$

where

$$\mathbf{X}(\mathbf{x},\,t) = \mathbf{x} - \int_{t}^{t^{n+1}} \mathbf{u}(\mathbf{X}(\mathbf{x},\,t'),\,t')\,dt' \tag{3.41}$$

is a Lagrangian position variable. It is then clear from (3.40) that the left-hand side of (3.32) is, indeed, an approximation to the substantial derivative, that is, an approximation to the space-time derivative following a material point in the fluid. As a corollary, we note that, in the steady state, the left-hand side of (3.32) is a streamline-upwind approximation to the convective term (Brooks and Hughes, 1982), with $O(\Delta t)^Q$ errors in streamline integration of the diffusive terms committed in (3.32), and $O(\Delta t)^4$ errors in characteristic-foot location and dispersion committed in (3.34)–(3.36).

The Backward-Differentiation/Runge–Kutta method is similar to two methods previously proposed for the treatment of the Navier–Stokes equations. First, from the Lagrangian interpretation, (3.37)–(3.41), the method can be viewed as a "characteristic" scheme of the variety introduced by Ewing and Russell (1981), Pironneau (1982), and Benqué, Ibler, Keramsi, and Labadie (1982). Second, from the subproblem treatment, (3.34)–(3.36), the method can be considered to be a "subcycle" technique, as described in Gresho, Chan, Lee, and Upson (1984). The relationship between these two methods has not, to our knowledge, been previously recognized. The merit of the operation-integration-factor derivation approach lies in the efficient, systematic extension of these concepts to higher-order discretizations; from the upwind arguments of the preceding paragraph, high-order methods for convection-Stokes splitting should be considered a necessity.

Remark 4. The operator-integration-factor approach presented in the current article arose, in fact, through recognition of (3.40) and subsequent generalization. Analyses of these pre-operator-integration-factor convection-Stokes "characteristic" methods may be found in Ho, Maday, Patera, and Rønquist (1990).

3.2.3. Numerical Results

In this section we consider solution of several two-dimensional problems by the Backward-Differentiation/Runge–Kutta method. To

completely characterize (3.32), (3.33) we need to specify the spatial discretization and Stokes solver: the spatial discretization will be taken to be the Legendre "$\mathbf{P}_N \times \mathbf{P}_{N-2}$" spectral element approximation (Maday, Patera, and Rønquist, 1987; Rønquist, 1988; Maday and Patera, 1989) characterized by K, the number of spectral elements, and N, the order of the polynomial approximation in each element in each spatial direction; the Stokes system will be solved by the Uzawa procedure described in Sec. 3.1.1 (see Remark 3).

To begin, we consider a simple model problem proposed by Kim and Moin (1985). The governing equations (3.27)–(3.29) are solved with $\rho = 1$ and $\nu = 1/2\pi^2$ in a domain Ω defined by $-1 \leqslant x \leqslant 1$, $-1 \leqslant y \leqslant 1$. The velocity $\mathbf{u} = u_1(x, y, t)\,\mathbf{i} + u_2(x, y, t)\,\mathbf{j}$ and pressure p are required to be 2-periodic in x and y. The initial conditions are taken to be

$$u_{1\,0}(x, y) = -\cos \pi x \sin \pi y \tag{3.42}$$

$$u_{2\,0}(x, y) = \sin \pi x \cos \pi y \tag{3.43}$$

for which the exact solution is then given by

$$u_1(x, y, t) = (-\cos \pi x \sin \pi y)\, e^{-t} \tag{3.44}$$

$$u_2(x, y, t) = (\sin \pi x \cos \pi y)\, e^{-t} \tag{3.45}$$

$$p(x, y, t) = -(\cos 2\pi x + \cos 2\pi y)\, e^{-2t}/4 \tag{3.46}$$

In order to investigate temporal convergence the solution is integrated to a time $T = 1.0$ with different Δt; N is maintained sufficiently large ($N = 12$) to ensure no spatial contamination of the error. We have also confirmed exponential convergence in space with increasing N (for sufficiently small Δt). In all cases $K = 4$ spectral elements are used.

We plot in Fig. 2 the velocity error in the H^1 norm at time $T = 1.0$ as a function of Δt for $Q = 1, 2, 3$. As expected, the Backward-Differentiation/Runge–Kutta method is Qth-order accurate. We note that for $Q = 3$ and at $\Delta t = 0.1$ ($\sigma = 16$) the realized speedup over our reference standard semi-implicit method is $\mathscr{S}' = 8$. [See Sec. 2.2.3 for definitions of σ, $\mathscr{S}$, and $\mathscr{S}'$; for this Navier–Stokes application $\Delta t_{\mathrm{cr,ref}}$ derives from the usual Courant condition, with a Courant number $C \equiv \max_{\Omega}(|\mathbf{u}|\, \Delta t_{\mathrm{cr,ref}}/\text{"}\Delta x\text{"}) = 0.25$ for our reference standard semi-implicit (Backward-Differentiation/Adams–Bashforth) method (Rønquist, 1988). Owing to the larger absolute stability region of the fourth-order Runge–Kutta scheme as compared to the third-order Adams–Bashforth scheme, we choose $\Delta s = \min\{\Delta s_{\mathrm{cr}} = 4\Delta t_{\mathrm{cr,ref}}, \Delta t\}$ in (3.34).] Although the solution (3.42)–(3.46) is admittedly simple, this example nevertheless demonstrates

the potential of the method to permit large effective time steps while simultaneously achieving high accuracy through higher-order discretizations. The large speedup is due to the fact that, in standard semi-implicit treatment of the Navier–Stokes equations, the stability-determining and work-intensive operators do not coincide.

As our second test case we consider a steady Navier–Stokes solution proposed by Kovasznay (1948). The governing equations (3.27)–(3.29) are solved with density unity and viscosity $\nu = 1/40$ in a domain Ω defined by $-1/2 \leqslant x \leqslant 1$, $-1/2 \leqslant y \leqslant 3/2$. The velocity $\mathbf{u} = u_1(x, y, t)\,\mathbf{i} + u_2(x, y, t)\,\mathbf{j}$ and pressure p are required to be 1-periodic in y; on $x = -1/2$ and $x = 1$

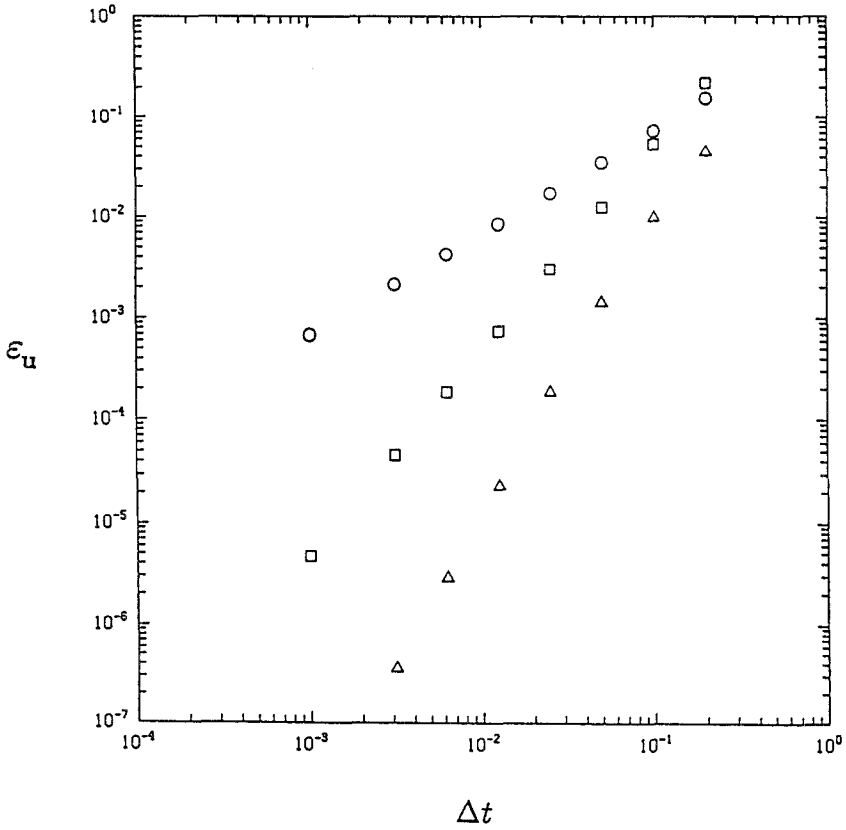

Fig. 2. The velocity error measured in the H^1-norm, ε_u, at time $T = 1.0$ as a function of the time step Δt for solution of the two-dimensional, unsteady Navier–Stokes equations (3.27), (3.28) subject to initial conditions given by (3.42), (3.43). The results are obtained using the Backward-Differentiation/Runge–Kutta method (3.32)–(3.36) for $Q = 1$ (○). $Q = 2$ (□), an $Q = 3$ (△).

we impose Dirichlet boundary conditions consistent with the exact steady (and two-dimensionally stable) solution,

$$u_1(x, y) = 1 - e^{\lambda x} \cos 2\pi y \tag{3.47}$$

$$u_2(x, y) = \lambda e^{\lambda x} \sin 2\pi y / 2\pi \tag{3.48}$$

$$p(x, y) = (1 - e^{2\lambda x})/2 \tag{3.49}$$

where $\lambda = 1/2\nu - (1/4\nu^2 + 4\pi^2)^{1/2}$. The streamlines of this solution are depicted in Fig. 3. In order to investigate "temporal" convergence the

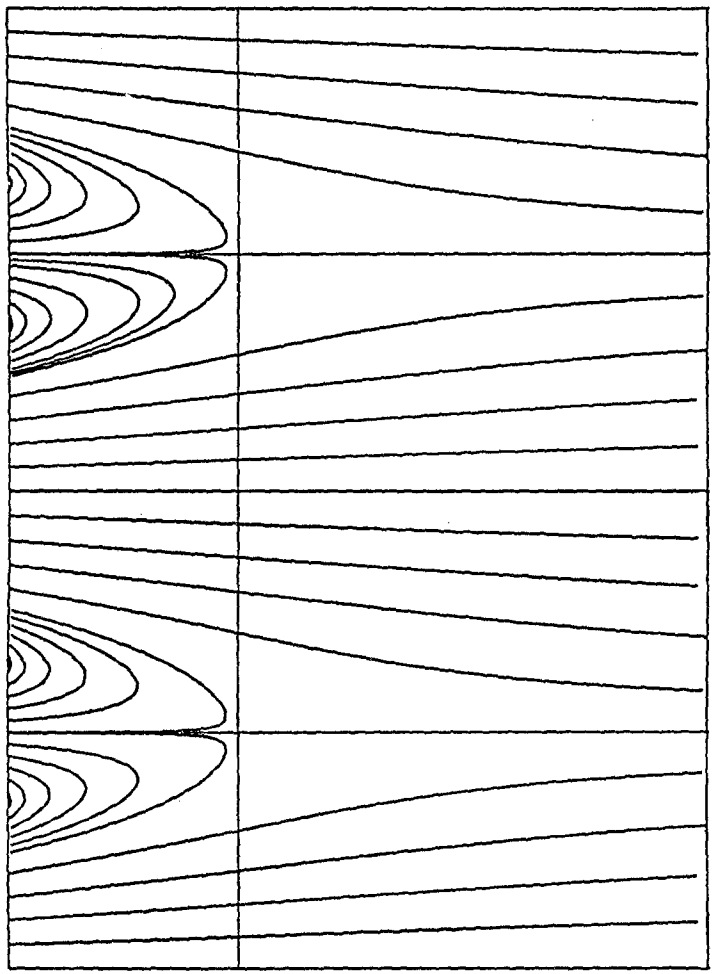

Fig. 3. Steady state streamline pattern for the Kovasznay (1948) flow for viscosity $\nu = 1/40$.

solution is integrated to a steady state with different Δt; N is maintained sufficiently large ($N = 11$) to ensure no spatial contamination of the error. Note that since the Backward-Differentiation/Runge–Kutta method is a splitting technique, "temporal" errors remain even at steady-state; from the discussion of the previous section, we recognize these error as errors in the upwind approximation of the convection terms. In all cases we use $K = 8$ spectral elements.

We plot in Fig. 4 the velocity error in the relative H^1 norm at steady state as a function of Δt for $Q = 1, 2, 3$. As for the periodic test problem, the Backward-Differentiation/Runge–Kutta method is Qth-order accurate. The positive effect of increasing the order of the scheme is again pronounced, with a several order-of-magnitude difference between the error in the $Q = 1$

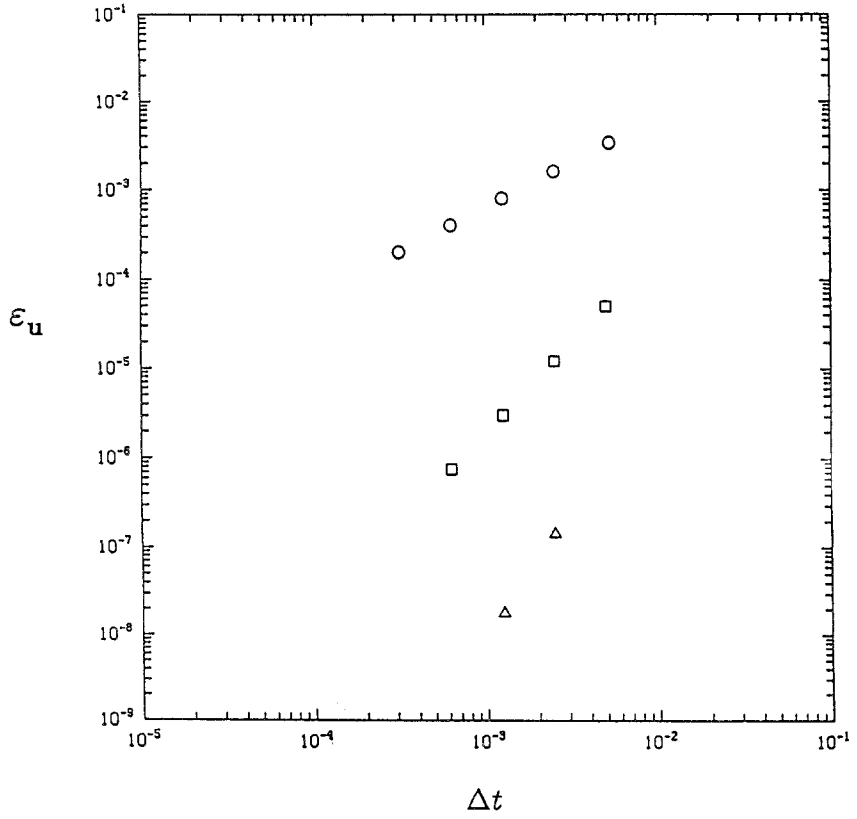

Fig. 4. The steady-state velocity error measured in the relative H^1-norm, ε_u, as a function of the time step Δt for solution of the two-dimensional Navier–Stokes equations (3.27), (3.28) with exact solution given by (3.47)–(3.49). The results are obtained using the Backward-Differentiation/Runge–Kutta method (3.32)–(3.36) for $Q = 1$ (○), $Q = 2$ (□), and $Q = 3$ (△).

(first-order upwind) and $Q=3$ approximations at the largest time step, $\Delta t=5\times10^{-3}$. For this problem the maximum speedup over our reference standard semi-implicit method is $\mathscr{S}'\approx3$; for larger Δt the scheme is unstable. The instability is caused by "nonlinear" aggravation of discontinuities in derivative propagated into the computational domain by the inviscid convection subproblem; these discontinuities originate in the nonzero normal derivative of the velocity, (3.47), (3.48), at inflow ($x=-1/2$). In practice this problem should arise only infrequently, as physical problems approximated by Dirichlet inflow boundary conditions will have small normal derivative at inflow if the artificial inflow boundary is sufficiently far "upstream." [Note that nonzero Dirichlet conditions are imposed on the *hyperbolic* subproblem (3.34)–(3.56) only on those segments of the boundary $\partial\Omega$ for which $\mathbf{u}\cdot\mathbf{n}<0$, where $\mathbf{n}$ is the outward normal on Ω; no boundary conditions are imposed where $\mathbf{u}\cdot\mathbf{n}\geqslant0$.]

Lastly, we consider the "real" problem of unsteady two-dimensional moderate-Reynolds-number flow in a periodic eddy promoter channel (Karniadakis, Mikic, and Patera, 1988). The governing equations (3.27)–(3.29) are solved in the domain Ω shown in Fig. 5a, with $d/h=0.4$, $b/h=0.5$, and $L/h=6.666$. The velocity $\mathbf{u}=u_1(x,y,t)\,\mathbf{i}+u_2(x,y,t)\,\mathbf{j}$ is required to be L-periodic in x, and to satisfy no-slip boundary conditions on the cylinder and channel walls. The pressure is written as

$$p(x,y,t)=\tilde{p}(x,y,t)-\overline{\frac{dp}{dx}}\,x \tag{3.50}$$

where $\tilde{p}(x,y,t)$ is L-periodic in x, and $\overline{dp/dx}$ is a constant driving force independent of time and space. [Note that our calculations here differ from those in Karniadakis, Mikic, and Patera (1988) in that the latter are at constant flowrate, not constant pressure gradient.] At a Reynolds number of $R=(\overline{dp/dx})\,h^3/2\rho\nu^2\approx140$ the flow undergoes a supercritical Hopf bifurcation to a (two-dimensionally) stable steady-periodic state with nondimensional period T_p (equal to the dimensional period normalized by $2\rho\nu/(h\,\overline{dp/dx})$). Our test problem is for $R=540$, with all calculations carried out to sufficiently long time to achieve a steady-periodic state. The $K=33$, $N=7$ spectral element spatial decomposition is shown in Fig. 5a.

We show in Fig. 5b the streamlines of the Backward-Differentiation/Runge–Kutta solution with $Q=3$ and $\Delta t=0.35$ ($\sigma=40$) at $R=540$ at one time in the steady-periodic cycle. [The time steps quoted are nondimensional, normalized by $2\rho\nu/(h\,\overline{dp/dx})$.] The simulation predicts a period of $T_p=14.38$, which is within .2% of the "exact" period $T_{p,\mathrm{ref}}=14.35$ obtained in a high-resolution (in space and time) reference calculation. The method achieves a realized speedup of $\mathscr{S}'\approx14$. A second

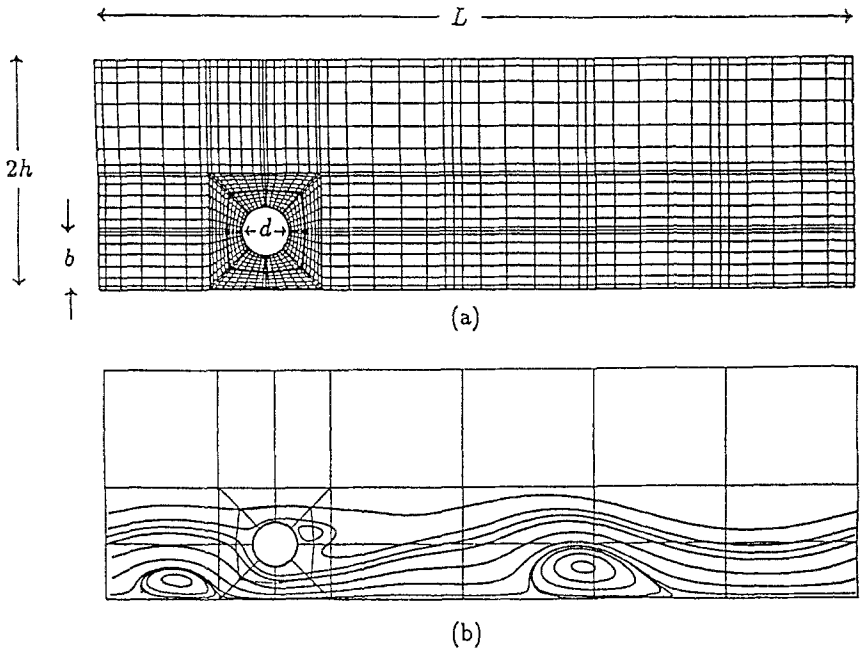

Fig. 5. Unsteady two-dimensional moderate-Reynolds-number flow in a periodic eddy promoter channel (Karniadakis, Mikic, and Patera, 1988). The Navier–Stokes equations (3.27), (3.28) are solved in a domain Ω shown in (a) with $d/h = 0.4$, $b/h = 0.5$, and $L/h = 6.666$ at a Reynolds number $R = (\overline{dp/dx})\, h^3/2\rho\nu^2 = 540$. The calculations are performed using the $K = 33$, $N = 7$ spectral element mesh shown in (a) combined with the $Q = 3$, $\sigma = 40$ Backward-Differentiation/Runge–Kutta temporal scheme described in (3.32)–(3.36). The streamlines at one time in the steady-periodic cycle are shown in (b).

calculation performed with $Q = 2$ and $\Delta t = 0.17$ ($\sigma = 20$) predicts $T_p = 14.44$, with a realized speedup of $\mathscr{S}' \approx 10$; this lower-order calculation is both slower *and* less accurate than the $Q = 3$ simulation, demonstrating the merit of high-order approximation of moderate-Reynolds-number flows.

We note that the Backward-Differentiation/Runge–Kutta method applied to the eddy-promoter problem will be unstable for sufficiently large Δt. This instability can be understood as follows: during the inviscid convection subproblem, (3.37)–(3.39), viscous normal boundary layers in $\mathbf{u}(\mathbf{x}, t^n)$ are steepened in proportion to Δt, with no mechanism for viscous saturation—this will occur, for example, on the upstream face of the eddy-promoter cylinder in Fig. 5. Upon temporal and spatial discretization, (3.34)–(3.36), this steepening tendency will be manifested, for sufficiently large Δt, or equivalently, sufficiently low spatial resolution, in the generation of spatial oscillations, or wiggles. These wiggles then lead to breakdown through the nonlinear coupling of the convection operator. The

steepening phenomenon places a fundamental limitation on the computational savings possible with pure-convection subcycling.

The eddy-promoter calculations indicate the potential of the Backward-Differentiation/Runge–Kutta method to accurately simulate real fluid flows; indeed, the method has been applied to numerous other two- and three-dimensional Navier–Stokes and natural convection problems with similar success. The two major problems with the method are: first, resolution difficulties arising from the purely inviscid nature of the convection subproblem; second, as currently formulated, the efficient divergence-form Stokes splitting methods of Sec. 3.1 cannot be exploited in (3.32). Numerous potential solutions exist to these problems, one of which will be described in the next section.

Remark 5. We have also applied the Backward-Differentiation/Runge–Kutta method with a Legendre $\mathbf{P}_N \times \mathbf{P}_N$ spectral element discretization of the Poisson (rather than divergence) form of the Navier–Stokes equations (Karniadakis), and the classical first-order invisicid-boundary-condition Poisson splitting scheme described in Sec. 3.1.4 (Chorin, 1970; Temam, 1984; Orszag, Israeli, and Deville, 1986). The resulting method behaves in a fashion similar to the divergence-discretization/Uzawa solver method described above, save that: $\mathscr{S}'/\mathscr{S}$ is lower, given the greater efficiency of the split-Poisson solvers as compared to Uzawa iteration; the larger Δt results are less accurate, in that the first-order Stokes splitting errors dominate.

4. CLOSING REMARKS

We restrict our closing remarks to two comments, the first an extension of the basic operator-integration-factor concept, the second a current limitation. As regards the former, it is clearly of interest to extend the operator-integration-factor splitting approach from two operators to many operators, that is, to consider methods for decomposition of the system,

$$\frac{d\underline{u}}{dt} = \sum_{p=1}^{P} \underline{A}_p(t)\,\underline{u} + \underline{f}(t), \qquad 0 < t < T \tag{3.51}$$

into P decoupled subproblems, each subproblem involving only a single operator $\underline{A}_p$. This decomposition is readily achieved; the operator-integration-factor approach, (2.1), (2.5)–(2.7), is intrinsically recursive, permitting high-order nested splitting methods to be constructed through repeated application of the integration-factor/subproblem process. One example of multioperator splitting germane to problems addressed in this article is a three-operator pressure–diffusion–convection nested decomposition of the

Navier–Stokes equations. This decomposition would partially alleviate the problems associated with the convection-subcycling scheme of the Sec. 3.2 by permitting controlled diffusion between pressure solves, thereby softening the inviscid effects of the convection step, and by permitting the methods of Secs. 3.1 and 3.2 to be used in concert.

We now turn to a significant limitation of the current operator-integration-factor approach as applied to partial differential equations. We note that the continuous-in-space analogues to (2.5) and (2.6) will have an initial-condition–boundary-condition incompatibility at $s=0$ in that, unless $Av=0$ on $\partial\Omega$ for all admissible v ($\equiv$ "Hypothesis A"), $d\tilde{\psi}/ds$ on $\partial\Omega$ from (2.5) will be inconsistent with the value imposed by (say) homogeneous Dirichlet boundary conditions. In essense, whereas in the unsplit equations u adjusts itself so that $Au+Bu+f=0$ does vanish on $\partial\Omega$ after a singular transient, by eliminating $Bu+f$ from (2.7) we reintroduce this transient, and singularity, at every time step. Low-order convergence results.

The results of this paper can be understood in light of these remarks as follows. First, the high-order convergence of the Crank–Nicholson scheme is due only to fortuitous cancellation. The Stokes splitting does not honor Hypothesis A, and, as expected, other high-order choices for S_A and S_B do not yield high-order convergence. Second, the convection-Stokes splitting *does* honor Hypothesis A owing to the appearance of the (vanishing) velocity in front of the gradient operator, thus explaining the very good "characteristic" results. We note that at inflow Hypothesis A is not exactly satisfied, perhaps causing the difficulties described in Sec. 3.2.3.

Numerous approaches are possible to eliminate the requirement of Hypothesis A; future work will address which, if any, of these techniques will prove practical and stable.

ACKNOWLEDGMENTS

We would like to thank Professor Gil Strang for helpful suggestions and comments. This work was supported by the ONR and DARPA under contract No. N00014–89-J-1610, by the ONR under contract No. N00014-88-K-0188, by the NSF under grant No. ASC-8806925, by the NSF/CNRS under grant No. INT-8914984, and by Nektonics Research Corporation.

REFERENCES

Adams, R. A. (1975). *Sobolev Spaces*, Academic Press, New York.

Ames, W. F. (1977). *Numerical Methods for Partial Differential Equations*, Academic Press, New York.

Arrow, K., Hurwicz, L., and Uzawa, H. (1958). *Studies in Nonlinear Programming*, Stanford University Press, Stanford.

Benqué, J. P., Ibler, B., Keramsi, A., and Labadie, G. (1982). A new finite element method for Navier–Stokes equations coupled with a temperature equation, in *Proc. 4th Int. Symp. on Finite Elements in Flow Problems*, Kawai, T. (ed). North-Holland, Amsterdam, pp. 295–301.

Bristeau, M. O., Glowinski, R., and Periaux, J. (to appear). Numerical methods for the Navier–Stokes equations. Applications to the simulation of compressible and incompressible viscous flows. *Comput. Phys. Rep.*

Brooks, A. N., and Hughes, T. J. R. (1982). Streamline upwind/Petrov–Galerkin formulations for convection dominated flows with particular emphasis on the incompressible Navier–Stokes equations, *Comput. Methods Appl. Mech. Eng.* **32**, 199–259.

Bussing, T. R. A., and Murman, E. M. (1988). Finite volume method for the calculation of compressible chemically reacting flows, in *AIAA J.* **26**, 1070–1078.

Cahouet, J., and Chabard, J. P. (1988). Some fast three-dimensional finite element solvers for the generalized Stokes problem, *Int. J. Numer. Methods Fluids* **8**, 869–895.

Canuto, C., Hussaini, M. Y., Quarteroni, A., and Zang, T. A. (1988). *Spectral Methods in Fluid Dynamics*. Springer-Verlag, Berlin.

Chao, Y., and Attard, A. (1985). A resolution of the stiffness problem of reactor kinetics, *Nucl. Sci. Eng.* **90**, 40–46.

Chorin, A. J. (1970). Numerical solution of incompressible flow problems, in *Studies in Numerical Analysis 2*, Ortega, J. M., and Rheinboldt, W. C. (eds.), SIAM, Philadelphia.

Deville, M. O., Kleiser, L., and Montigny-Rannou, F. (1984). Pressure and time treatment for Chebyshev spectral solution of a Stokes problem, *Int. J. Methods Fluids* **4**, 1149.

Douglas, J., Jr. (1955). *SIAM* **3**, 42.

Ewing, R. E., and Russell, T. F. (1981). Multistep Galerkin methods along characteristics for convection–diffusion problems, in *Advances in Computer Methods for Partial Differential Equations–IV*, Vichnevetsky, R., and Stepleman, R. S. (eds.), IMACS, Rutgers University, New Brunswick, New Jersey, pp. 28–36.

Gear, C. W. (1971). Numerical Initial Value Problems in Ordinary Differential Equations, Prentice-Hall, Englewood Cliffs, New Jersey.

Gear, C. W. (1980). Automatic multirate methods for ordinary differential equations, *International Federation for Information Processing*, North-Holland, Amsterdam.

Girault, V., and Raviart, P. A. (1986). *Finite Element Approximation of the Navier–Stokes Equations*, Springer-Verlag, Berlin.

Glowinski, R. (1984). *Numerical Methods for Nonlinear Variational Problems*, Springer-Verlag, Berlin.

Golub, G. H., and Van Loan, C. F. (1983). *Matrix Computations*, John Hopkins University Press, Baltimore, Maryland.

Gresho, P. M., Chan, S. T., Lee, R. L., and Upson, C. D. (1984). A modified finite element method for solving the time-dependent, incompressible Navier–Stokes equations, Part 1: Theory, *Int. J. Numer. Methods Fluids* **4**, 557–598.

Friesner, R. A., Tuckerman, L. S., Dornblaser, B. C., and Russo, T. V. (to appear). A method for exponential propagation of large systems of stiff nonlinear differential equations, in Proceedings of the Second Nobeyama Workshop on Supercomputers and Fluid Dynamics (Japan, 1989), *J. Sci. Comput.*

Ho, L. W. (1989). A Spectral Element Stress Formulation of the Navier–Stokes Equations, Ph.D. thesis, Massachusetts Institute of Technology, Cambridge.

Ho, L. W., Maday, Y., Patera, A. T., and Rønquist, E. M. (1990). A high-order Lagrangian-decoupling method for the incompressible Navier–Stokes equations, *Comput. Methods Appl. Mech. Eng.* (to appear).

Ho, L. W., and Patera, A. T. (1990a). A Legendre spectral element method for simulation of

unsteady incompressible viscous free-surface flows, *Comput. Methods Appl. Mech. Eng.* (to appear).

Ho, L. W., and Patera, A. T. (1990b). Variational formulation of three-dimensional viscous free-surface flows: Natural imposition of surface tension boundary conditions, *Int. J. Numer. Methods Fluids* (to appear).

Hofer, E. (1976). A partially implicit method for large stiff systems of ODE's with only a few equations introducing small time-constants, *SIAM J. Numer. Anal.* **13**(5), 645.

Karniadakis, G. E. (to appear). Spectral element simulations of laminar and turbulent flows in complex geometries, *Appl. Numer. Math.*

Karniadakis, G. E., Israeli, M., and Orszag, S. A. (submitted). High-order splitting methods for the incompressible Navier–Stokes equations. *J. Comput. Phys.*

Karniadakis, G. E., Mikic, B. B., and Patera, A. T. (1988). Minimum-dissipation transport enhancement by flow destabilization: Reynolds' analogy revisited, *J. Fluid Mech.* **192**, 365–391.

Kim, J., and Moin, P. (1985). Application of a fractional-step method to incompressible Navier–Stokes equations, *J. Comput. Phys.* **59**, 308–323.

Kovasznay, L. I. G. (1948). Laminar flow behind a two-dimensional grid. In *Proc. Cambridge Phil. Soc.* **44**, 58–62.

Maday, Y., Meiron, D., Patera, A. T., and Rønquist, E. M. (submitted). Analysis of iterative method for the steady and unsteady Stokes problem: Application to spectral element discretizations.

Maday, Y., and Patera, A. T. (1989). Spectral element methods for the incompressible Navier–Stokes equations, in *State of the Art Surveys in Computational Mechanics*, Noor, A. K. (ed.). ASME, New York, pp. 71–143.

Maday, Y., Patera, A. T., and Rønquist, E. M. (1987). A well-posed optimal spectral element approximation for the Stokes problem, ICASE Report No. 87–48.

Marchuk, G. (1971). On the theory of the splitting method. In *Numerical Solution of Partial Differential Equations II*, Hubbard, B. (ed). Academic Press, New York, p. 469.

Orszag, S. A., Israeli, M., and Deville, M. O. (1986). Boundary conditions for incompressible flows, *J. Sci. Comput.* **1**, 75.

Palusinski, O. A., and Wait, J. V. (1978). Simulation methods for combined linear and non-linear systems, *Simulation* **30**(3), 85–94.

Peaceman, D. W., and Rachford, H. H., Jr. (1955). *SIAM* **3**, 28.

Pironneau, O. (1982). On the transport-diffusion algorithm and its applications to the Navier–Stokes equations, *Numer. Math.* **38**, 309–332.

Rogallo, R. S. (1977). An ILLIAC Program for the Numerical Simulation of Homogeneous Incompressible Turbulence. NASA TM-73203.

Rønquist, E. M. (1988). Optimal Spectral Element Methods for the Unsteady Three-Dimensional Incompressible Navier–Stokes Equations, Ph.D. Thesis, Massachusetts Institute of Technology, Cambridge.

Saleh, R. A., and Newton, A. R. (1989). The exploitation of latency and multirate behavior using nonlinear relaxation for circuit simulation, *IEEE Trans. Computer-Aided Design* **8**(12), 1286–1298.

Spalart, P. R. (1986). Numerical Simulation of Boundary Layers, Part 1: Weak Formulation and Numerical Method, NASA TM-88222.

Strang, G. (1968). On the construction and comparison of difference schemes, *SIAM J. Numer. Anal.* **5**(3), 506–517.

Strang, G. (1990). Private communication.

Temam, R. (1984). *Navier–Stokes Equations, Theory and Numerical Analysis*, North-Holland, Amsterdam.

Vandeven, H. (1990). Analysis of the eigenvalues of spectral differentiation operators, in Proceedings of the International Conference on Spectral and High-Order Methods for Partial Differential Equations, *Comput. Methods Appl. Mech. Eng.* (to appear).

Weidemann, J. A. C., and Trefethen, L. N. (1990). The eigenvalues of second-order spectral differentiation matrices. *SIAM J. Numer. Anal.* (to appear).

White, J., and Vincentelli, A. S. (1987). *Relaxation Techniques for the Simulation of VLSI Circuits*, Kluwer Academic Press, Boston.

Yanenko, N. N. (1971). *The Method of Fractional Steps*, Springer, New York.

Zang, T. A., and Hussaini, M. Y. (1986). On spectral multigrid methods for the time-dependent Navier–Stokes equations, *Appl. Math. Comput.* **19**, 359–372.